Journal of Magnetics 17(3), 219-224 (2012) http://dx.doi.org/10.4283/JMAG.2012.17.3.219

Changes in SNR and ADC According to the Increase in b Value in Liver Diffusion-Weighted Images

Jae-Hwan Cho[1,2] and Ham-Gyum Kim[3]*

[1]*Department of International Radiological Science, Hallym University of Graduate Studies, Seoul 135-841, Korea*
[2]*Department of Computer Science and Engineering, Soonchunhyang University, Asan 336-745, Korea*
[3]*Department of Radiological Technology, Ansan College, Ansan 426-701, Korea*

(Received 17 May 2012, Received in final form 6 June 2012, Accepted 11 June 2012)

In the present study, changes in signal-to-noise ratio (SNR) and apparent diffusion coefficient (ADC) of the diffusion-weighted images in the normal livers were investigated using changes in b values in 1.5 T MR (magnetic resonance) instruments. Respective diffusion-weighted images and ADC map images were obtained from 20 healthy individuals by increasing b values from 50 to 400 and 800 s/mm^2 using 1.5T MR scanner between January 2011 and November 2011. At each ADC map image obtained at each b value, ADCs in the right hepatic lobe, spleen and kidney were measured. As a result, ADCs of the right hepatic lobe, spleen and kidney have gradually decreased in the diffusion-weighted images in accordance with the reduced b value. This outcome may be used as preliminary data for applications to various abdominal diseases.

Keywords : liver, diffusion-weighted imaging, ADC map images, b value, ADC

1. Introduction

By virtue of the rapid advancements in MR hardware and software technologies, excellent images with less virtual images having adequate CNR for detection and diagnosis of pathologies have become available in a short period of time. Accordingly, MRI has been recognized as a useful method for detection and differentiation diagnosis of liver diseases, and now replaces CT scan in many areas of diagnosis and evaluation after treatments of liver diseases. Liver lesions in MR images without contrast enhancement are not clearly observed due to the low liver tissue to lesion ratio. Therefore, developments of tissue-specific contrast agents for detection and specification of liver diseases have been under process [1, 2].

In particular, gadoxetate (Gd-EOB-DTPA) which is a liver cells-specific contrast agent has drawn attention because functional images of liver cells as well as the dynamic images with non-specific extracellular contrast agents can be obtained. Gadoxetate provides not only additional diagnostic values in the specification of local lesions of the liver, but a better performance in the detection of liver cancer compared with multidetector CT scan [3].

Liver MRI obtains contrast enhancement 3-dimensional T1 weighted images using gadolinium agents. In addition, chemical shift T1 weighted images and T2 weighted images composed of in-phase and opposed-phase are also obtained. More recently, diffusion-weighted imaging is widely used as a routine protocol [4, 5]. Diffusion-weighted imaging is an MR technique visualizing diffusion features of water molecules in tissues, which can help detection and differentiation diagnosis of liver focal lesions. Diffusion-weighted imaging is a technique visualizing water movements in and out of cellular spaces, and is useful to detect the focal lesions in the liver [6]. In order to obtain diffusion-weighted images, a pair of very strong gradient magnetic field meaning a diffusion-weighted gradient magnetic field is required as well as the typical gradient magnetic field which is used for obtaining ordinary images. Integral of strength and time of diffusion weighted gradient magnetic field is called gradient factor or b value [7], and the larger the gradient factor is, the more diffusion-weighted images can be obtained. The numerical expression of water diffusion is apparent diffusion coefficient (ADC) [8]. The b value which represents the strengths of the diffusion-weighted gradient magnetic field is widely used at 400 s/mm^2. However, we could not find any report on diffusion-weighted imaging according to the b Value in

*Corresponding author: Tel: +82-31-400-6942
Fax: +82-31-400-6939, e-mail: 8452404@hanmail.net

diffusion-weighted images. In the present study, effects of SNR and ADC on diffusion-weighted imaging in the healthy livers with 1.5 T MR instruments were investigated.

2. Means and methods

Images of 20 healthy livers were obtained using 1.5T MR scanner (Signa 1.5T HDx. GE Healthcare. Milwaukee. WI, USA) and HD T/R 8ch Torso array coil (In vivo Corp. Gainesville. FL, USA) between January 2011 and November 2011. Prior to conducting diffusion-weighted imaging, fat-suppressed T2 weighted images (TR=8000 msec, TE=91 msec, NEX=2) were obtained using fast spin-echo (FSE) imaging technique in order to observe anatomical structures (Fig. 1). With the b values at 50, 400 and 800 s/mm^2, 3 pairs of diffusion-weighted sagittal plane images were obtained using spin-echo EPI technique. Variables of images are as follows:

TR (time of repetition): 12000 ms, TE (time of echo): 75 ms, Matrix: 128×128, NEX (average): 2, Slice thickness: 5.0 mm, FOV (field of view): 360 mm

The acquired diffusion-weighted images were sent to Advantage Workstation (Ver 4.3, Revision 4. GE healthcare. Milwaukee. WI, USA) and then, ADC map images were obtained.

Usually in diffusion-weighted imaging, gradient pulses are applied as shown in Fig. 2.

A gradient pulse encodes the spins with a characteristic phase dependent on spatial position along the gradient direction, as depicted in Fig. 2. The equation that describes the amount of phase, φ, imparted on each spin after a gradient pulse is applied, on the x-axis for example, is given by [9]

Fig. 1. Fat-suppressed T2 weighted images using fast spin-echo (FSE) imaging.

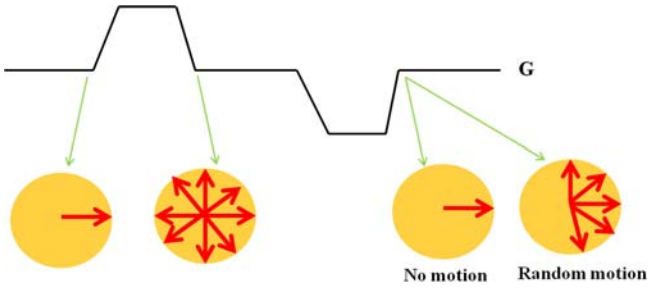

Fig. 2. (Color online) Before a diffusion gradient is applied, the spins within a voxel have identical phase. The first diffusion gradient encodes each spin with a phase dependant on its position. If no motion has occurred, the second diffusion gradient, that has the same strength and opposite polarity, will rewind the phase of each spin.

$$\phi = \gamma \int_0^t G(t') \times x(t') dt' \tag{1}$$

A second gradient of equal time and equal and opposite amplitude will remove the phase that was set up by the first gradient. For static spins, where no net translational movement has taken place, the phase of all the spins will be brought back together, as depicted in Fig. 2. If diffusion has occurred then some intravoxel phase dispersion will remain. Assuming movement only occurs between the gradients, with amplitude GD and duration δ, the change in phase, Δφ, for a spin that has moved an amount Δx can be calculated from EQ 2 to be [9]

$$\Delta\phi = \gamma\delta G_D \Delta x = q\Delta x \tag{2}$$

The result is an attenuation of the signal amplitude that is due to the destructive interference of the spins with varying phase. The following equation describes a general signal attenuation due to a distribution of phase [9]:

$$S = S_0 \int e^{i\Delta\phi} P(\Delta x) d\Delta x \tag{3}$$

where $P(\Delta x)$ is the probability distribution of the ensemble of diffusing spins. The Einstein relation states that for free diffusion, $P(\Delta x)$ is a Gaussian [9, 10]. Substituting in EQ 2 for $\Delta\varphi$ and assuming free diffusion, EQ 3 is written as [9]

$$S = \frac{S_0}{\sqrt{2\pi\sigma_{\Delta x}^2}} \int e^{iq\Delta x} e^{-\frac{(\Delta x)^2}{2\sigma_{\Delta x}^2}} d\Delta x \tag{4}$$

By way of the Fourier Transform, this integral solves to [9]

$$S = S_0 e^{-\frac{\frac{q^2}{2}\sigma_{\Delta x}^2}{2}} \tag{5}$$

$\sigma^2_{\Delta x}$ is the variance of the Gaussian probability function, and for free diffusion has the form [9]

$$\sigma^2_{\Delta x} = [\Delta x]^2 = 2DT_{diff} \quad (6)$$

The variance of the Gaussian is a function of both the diffusion coefficient, D, and the total amount of time spins are allowed to diffuse, Tdiff. Substituting Eq. (6) into Eq. (5) and writing out q in its full form, the equation for signal attenuation due to diffusion is given by [9]

$$S = S_0 e^{-(\gamma\delta G_D)^{2DT_{diff}}} \quad (7)$$

Stejskal and Tanner published a derivation for the effects of a time-dependent magnetic field gradient in the presence of spin diffusion [9, 11]. The Stejskal-Tanner sequence is based on a spin-echo sequence with the addition of two gradient pulses of duration δ and amplitude G_D that are separated by an observation, or diffusion, time Δ. The total amount of time spins are allowed to diffuse, Tdiff, used in the previous equations is the same as Δ. The spin-echo diffusion preparation is diagramed in Fig. 3 with a diffusion gradient applied to an arbitrary axis. Following the 90° RF excitation pulse, it is assumed there is no loss of phase coherence. The first diffusion gradient produces a phase shift that depends upon the position of each spin in the direction of the gradient. A 180° RF pulse then inverts the phase shifts caused by the first gradient pulse. The second diffusion gradient produces phase shifts equal to those produced by the first. If there is no net movement, the second gradient would exactly undo the effect of the first gradient. Diffusion causes the refocusing to be incomplete [9, 11]. The ratio of signals acquired with the gradients on and the gradients off, provides information about the average diffusion of the spins in the system. As seen in the provided derivation, the resultant signal attenuation is a function of the phase dispersion and the probability distribution. The equation for signal attenuation is most commonly described as [9]

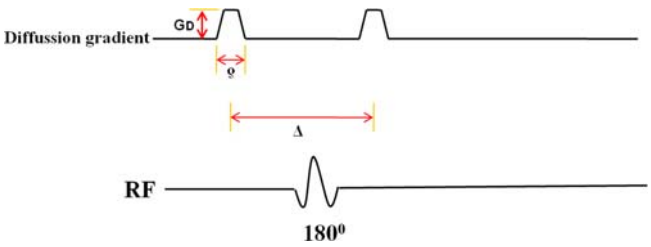

Fig. 3. (Color online) The length of the gradient pulses is denoted by δ with an amplitude equal to G_D. The space in between them, the diffusion time, is denoted by Δ. By employing a 180° RF, dephasing from T2† is reduced causing an increase in signal for data collection.

$$S = S_0 e^{-bD} \quad (8)$$

where S_0 is the net magnetization that would be obtained in the absence of diffusion or a non-diffusion-weighted dataset when GD=0 and

$$b = (\gamma\sigma G_D)^2\left(\Delta - \frac{\sigma}{3}\right) \quad (9)$$

If δ << Δ then (Δ–δ/3) becomes Δ and b has the same form of the exponent in Eq. (7) [9].

The equations derived above are for the MR signal, S. Intensity in an image, I, is generated from this signal. Because each voxel in an image may contain multiple types of tissue with water in both the intra- and extra-cellular spaces, the parameter that is measured in a diffusion experiment is called an apparent diffusion coefficient (ADC), rather than the true diffusion coefficient. The ADC can be calculated from two images, one with and one without diffusion weighting, by finding the slope of a natural log plot of $I(x,y)/I_0(x,y)$ [9]

$$ADC(X,Y) = -\frac{1}{b}\ln\left(\frac{I(x,y)}{I_0(x,y)}\right) \quad (10)$$

Many tissues, particularly in the brain, exhibit long-range microstructural order, which not only restricts water motion, but also imparts anisotropy to the translational motion of water, i.e. a directional dependence [9].

With the ADC map images obtained at each b value, ADCs at the right hepatic lobe and spleen and kidney were measured (Fig. 4).

As a quantitative analysis on the experiment, mean of ADCs was calculated, and images at each b value were

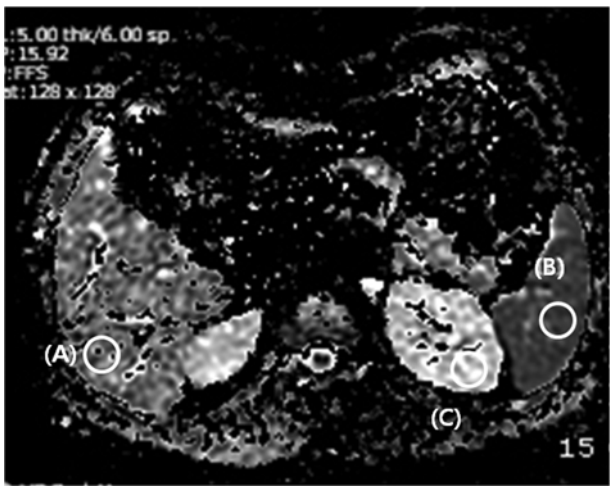

Fig. 4. At ADC map images obtained at each b value, ADCs of right hepatic lobe (A), spleen (B) and kidney (C) were measured.

Table 1. ADC changes in the right hepatic lobe in ADC map images by b values.

b value (s/mm^2)	50	400	800	P
right hepatic lobe (mm^2/s)	5.24 ± 1.01	1.62 ± 0.35	1.15 ± 0.22	0.025*
At 50 s/mm^2	1	0.30	0.21	

Table 2. ADC changes in the spleen in ADC map images by b values.

b value (s/mm^2)	50	400	800	P
right hepatic lobe (mm^2/s)	2.89 ± 1.34	1.03 ± 0.24	0.82 ± 0.19	0.043*
At 50 s/mm^2	1	0.35	0.28	

Table 3. ADC changes in the kidney in ADC map images by b values.

b value (s/mm^2)	50	400	800	P
right hepatic lobe (mm^2/s)	4.12 ± 2.24	2.21 ± 0.51	1.98 ± 0.34	0.020*
At 50 s/mm^2	1	0.53	0.48	

compared with the ADC map images obtained at 50 s/mm^2 of b value.

Difference in the mean of SNR and ADC at each b value was tested by ANOVA (SPSS win 16.0, USA), and for more accurate difference, post-hoc analysis was conducted ($p < 0.05$).

3. Results

As a result of the quantitative analysis, ADC of the right hepatic lobe increased in the ADC map images according to the increasing b value as shown in Table 1 ($P < 0.05$). When ADC was set at 1 in the ADC map images with the b value at 50 s/mm^2, the mean ADCs with the b value at 400 and 800 s/mm^2 reduced to 0.30 and 0.21, respectively (Table 1).

Spleen ADC decreased in accordance with the increasing b value as shown in Table 2 ($P < 0.05$). When ADC was set at 1 in the ADC map images with the b value at 50 s/mm^2, the mean ADCs with the b value at 400 and 800 s/mm^2 reduced to 0.35 and 0.28, respectively (Table 2).

ADC decreased in accordance with the increasing b Value as shown in Table 2 ($P < 0.05$). When ADC was set at 1 in the ADC map images with the b value at 50 s/mm^2, mean ADCs with the b value at 400 and 800s/mm^2 decreased to 0.53 and 0.48, respectively (Table 3).

In summary, in accordance with the increase in b value in the ADC map images, ADCs of the right hepatic lobe, spleen and kidney decreased (Figs. 5, 6).

4. Discussion

Diffusion-weighted imaging is a technique to observe molecular motions using the phase shift theory. About 70% of the water inside the body occupies an extracellular space which is only for water, and the rest 30%

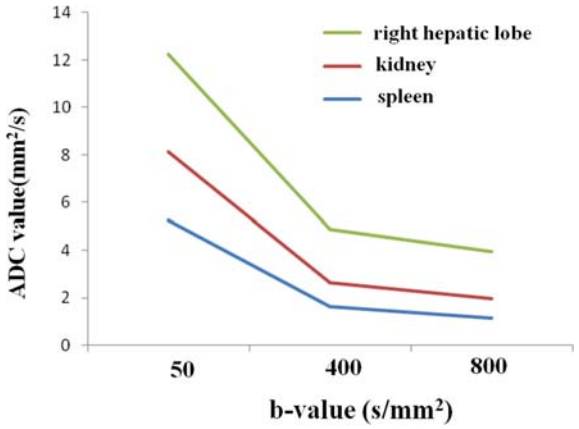

Fig. 6. (Color online) At ADC map images, ADCs of right hepatic lobe, spleen and kidney decreased in accordance with the increasing b values.

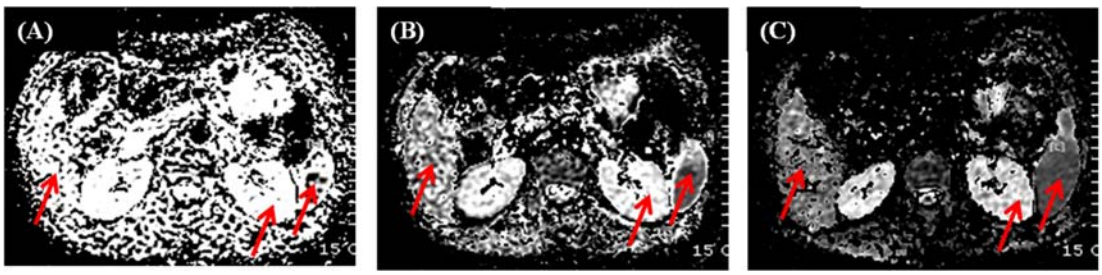

Fig. 5. (Color online) At ADC map images, ADCs of right hepatic lobe, spleen and kidney decreased in accordance with the increasing b values at 50 s/mm^2 (A), 400 s/mm^2 (B) and 800 s/mm^2 (C).

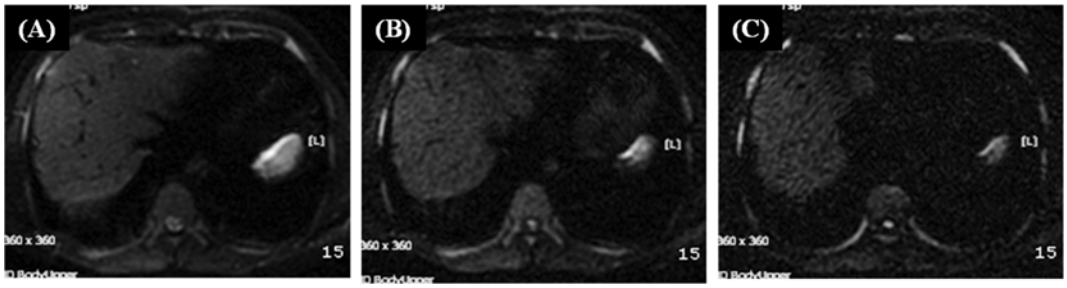

Fig. 7. At diffusion weighted image, signal strength decreased in accordance with the increasing b values at 50 s/mm^2 (A), 400 s/mm^2 (B) and 800 s/mm^2 (C).

remains in cells. Diffusion-weighted imaging shows the balance between the spaces in and out of the cells. When the balance is lost, difference in signal-strength is detected in diffusion-weighted imaging [12]. Since the usefulness of DWI for detection and characterization for liver focal lesions has been proved, it is widely used as a routine protocol [13].

In order to obtain diffusion-weighted images, a pair of very strong gradient magnetic field meaning a diffusion-weighted gradient magnetic field is required as well as the typical gradient magnetic field which is used for obtaining ordinary images. Integral of strength and time of diffusion-weighted gradient magnetic field is called gradient factor or b value. The larger the ADC of the tissues is, the larger the gradient factor is, and the more signal reduction by diffusion appears [14, 15]. In the present study, signal strengths in diffusion-weighted imaging according to changes in b value were not measured, but according to the qualitative analysis, signal strengths decreased in accordance with the increase in b value (Fig. 7). In cases of abdominal examinations, B value is usually set at 0 and 400 s/mm^2 for detection and characterization of lesions.

In diffusion-weighted imaging, ADCs can be obtained by calculating diffusion coefficient by pixel and then, through post-image processing. New images composed of ADC values are called ADC images, and they enable not only finding out lesions in various locations but quantitative analysis on ADC at the locations. Therefore, on this map, tissues with excellent diffusion are seen as a high signal, and tissues with poor diffusion are seen as a low signal, which are opposite to the signals of diffusion-weighted imaging [16].

In the precedent diffusion-weighted imaging studies, ADC was obtained mainly from lesions and consequently, benign cyst lesions showed high ADC values, while malignant solid lesions showed low ADC values [17, 18]. In the present study, ADCs in the right hepatic lobe, spleen and kidney of the healthy individuals without lesions were measured. Chris *et al.* [19] reported that ADCs in white and grey matters of the brain decreased in accordance with the increase in b value. In the present study, ADCs in ADC map images of the right hepatic lobe, spleen and kidney decreased in accordance with the increase in b value. In summary, ADCs of the right hepatic lobe, spleen and kidney have gradually decreased in the diffusion-weighted images accordance with the reduced b value. This outcome may be used as preliminary data for applications to various abdominal diseases.

5. Conclusion

ADCs of the right hepatic lobe, spleen and kidney have gradually decreased in the diffusion-weighted images accordance with the reduced b value. However, comparison on ADCs with b values was not clinically verified. Despite, recognition of signal changes in the diffusion-weighted imaging tests using multi b values in case of liver disease patients is considered important. The outcomes of the present study may be used as preliminary data for applications to various abdominal diseases.

References

[1] C. J. Fretz, D. D. Stark, C. E. Metz, G. Elizondo, R. Weissleder, J. H. Shen, J. Wittenberg, J. Simeone, and J. T. Ferrucci, Am. J. Roentgenol. **155**, 763 (1990).
[2] K. D. Hagspiel, K. F. Neidl, A. C. Eichenberger, W. Weder, and B. Marincek, Radiology **196**, 471 (1995).
[3] M. Strotzer, J. Gmeinwieser, J. Schmidt, C. Fellner, J. Seitz, H. Albrich, H. Zirngibl, and S. Feuerbach, Acta Radiol. **38**, 986 (1997).
[4] D. Le Bihan, E. Breton, D. Lallemand, M. L. Aubin, J. Vignaud, and M. Laval-Jeantet, Radiology **168**, 497 (1988).
[5] H. C. Thoeny and F. De Keyzer, Eur. Radiol. **17**, 1385 (2007).
[6] D. M. Koh and D. J. Collins, Am. J. Roentgenol. **188**, 1622 (2007).
[7] J. H. Lee, C. H. Sohn, and J. S. Choi, J. Korean Radiol. Soc. **49**, 455 (2003).

[8] D. Chien, K. K. Kwong, D. R. Gress, F. S. Buonanno, R. B. Buxton, and B. R. Rosen, AJNR **13**, 1097 (1992).
[9] J. E. Sarlls, "High-resolution diffusion-weighted magnetic resonance imaging: Development and application of novel radial fast spin-echo acquisitions", Ph. D. Thesis, The University of Arizona 3215376 (2006).
[10] A. Einstein, Investigations on the Theory of Brownian Motion. Dover, New York (1926).
[11] E. O. Stejskal and J. E. Tanner, J. Chem. Phys. **42**, 288 (1965).
[12] S. Warach, J. Gaa, B. Siewert, P. Wielopolski, and R. R. Edelman, Ann. Neurol. **37**, 231 (1995).
[13] B. Taouli and D. M. Koh, Radiology **254**, 47 (2010).
[14] M. C. DeLano, T. G. Cooper, J. E. Siebert, M. J. Potchen, and K. Kuppusamy, Am. J. Neuroradiol. **21**, 1830 (2000).
[15] J. H. Burdette, D. D. Durden, A. D. Elster, and Y. F. Yen, J. Comput. Assist. Tomogr. **25**, 515 (2001).
[16] T. Namimoto, Y. Yamashita, S. Sumi, Y. Tang, and M. Takahashi, Radiology **204**, 739 (1997).
[17] T. Kim, T. Murakami, S. Takahashi, M. Hori, K. Tsuda, and H. Nakamura, Am. J. Roentgenol. **173**, 393 (1999).
[18] T. Bachir, V. Valerie, D. Erik, D. Jean-Luc, F. Bo, and M. Yves, Radiology **226**, 71 (2003).
[19] C. A. Clark and L. B. Denis, Magnetic Resonance in Medicine **44**, 852 (2000).